JOURNAL OF PROPULSION AND POWER
Vol. 28, No. 5, September–October 2012

Technical Notes

Simulation of Plasma Parameters During Hollow Cathodes Operation

J. Mizrahi,* V. Vekselman,† V. Gurovich,‡ and Ya. E. Krasik§
Technion—Israel Institute of Technology, 32000 Haifa, Israel

DOI: 10.2514/1.B34406

Nomenclature

b_0 = impact parameter for coulomb collisions with a large scattering angle, m
c_v = specific heat capacity at constant volume for xenon gas, J/(kg °K)
c_{total} = specific heat capacity at constant volume per unit of volume for xenon plasma, $J/(m^3\ kg\ °K)$
D_i, D_a = ion and ambipolar diffusion coefficient, m^2/s
e = electron charge, C
F = mass flow rate, kg/s
I_e = electron current, A
I_i^{prod}, I_i^{loss} = ion production and loss rates, A
J_i^A, J_i^B = radially averaged axial ion current densities at the orifice input and output, A/m^2
J_i^w = ion current to the wall, A/m^2
k_B = Boltzmann constant, J/°K
L = orifice length, m
M = xenon atom mass, kg
m = electron mass, kg
m_{Xe} = xenon gas molar mass, kg/mol
n, $\bar{n}$ = plasma density and average plasma density, m^{-3}
n_0^A, n_0^B = neutral gas density at the input and exit of the orifice, m^{-3}
$\bar{n}_0$ = average neutral gas density, m^{-3}
$P_0^{A,B}$ = neutral gas pressure at the orifice input/exit (superscript A/B) of the orifice, Pa
Q_{ei}, Q_{en}, Q_{total} = electron—ion, electron—neutral, and total density of energy exchange rate, $J/(m^3\ s)$
$\tilde{R}$, R = ideal gas universal constant, J/(°K mol), and resistance of the plasma within the orifice, Ω
r = orifice radius, m
T_e, T_i, T_0 = electron, ion, and neutral gas temperature, eV
T_e^{ins} = average electron temperature in the insert region
T_r = reduced temperature
U_{ion}, U_{excit} = mean electron energy loss due to an ionization/excitation event, eV
u_0 = axial neutral gas velocity, m/s
$\bar{u}_e$, u_e^d = electron thermal and drift velocity, m/s
$u_i^{A,B}$ = radially averaged axial ion velocity at the input/exit of the orifice, m/s
α = ratio between neutral gas density (orifice outlet)/(orifice inlet)
η = plasma resistivity, V m/A
λ_{CEX}, λ_D = mean free path for charge exchange and debye length, m
μ_i, μ_e = ion and electron mobility.
ν_{ei}, ν_{en}, ν_{in} = electron—ion, electron—neutral, and ion—neutral collision frequencies, s^{-1}
ξ = neutral gas viscosity, Pa s
σ_{CEX}, σ_{ion}, σ_{en} = cross section for charge exchange, ionization by impact, and electron—neutral collisions, m^2
σ_{rad}, σ_{in} = cross section for excitation with radiative decay and ion—neutral collisions, m^2

I. Introduction

ION and Hall thrusters are promising propulsion systems for use in missions in space due to their high efficiency and low consumption of propellant. These types of thruster use a hollow cathode (HC) as a source of electrons for the ionization of the propellant and neutralization of the ion beam that produces the thrust (see Fig. 1).

Ion and Hall thrusters produce a low thrust and, therefore, they should operate for the thousands of hours required to accomplish a space mission. This implies that the lifetime of the HCs becomes a crucial issue especially for an HC with a small orifice diameter, which does not require a large gas flow rate but dictates a high pressure and a low electron plasma temperature in the insert region. The high pressure results in a low plasma potential, which in turn reduces the energy of the ions reaching the insert wall. The latter prevents the severe erosion of the insert, thus increasing the lifetime of the HC. In addition, because the plasma within the small-size orifice is rather resistive, significant plasma joule heating and power deposition in the orifice wall is realized. The latter results in heat transfer to the insert by radiation and conduction, enabling the HC to operate in a self-heating mode.

Measuring the plasma parameters inside these types of HC is a problematic issue because of the small orifice dimensions and high current density (10^2–10^3 A/cm^2) [1]. Modeling of the plasma behavior inside the orifice can therefore give insight about the HC's performance.

In this paper, a zero-dimensional (0-D) model for the plasma within the orifice of an HC with a large aspect ratio $L/(2r)$ is considered. This model takes into account nonuniform distributions of some of the plasma parameters, and the resulting set of algebraic equations describes the behavior of the averaged plasma parameters.

II. Description of the Model

The model is based on charged particle flows and energy balances coupled with a model for the neutral gas flow. The plasma within the orifice is assumed to have azimuthal symmetry, and the values T_e, T_0, I_e, and u_0 are assumed to be constant within the orifice. Also, there is no radial variation in n_0 and u_i; however, these two parameters vary in the axial direction. The plasma density n varies in the axial and radial directions $n(r, z)$, but its gradients determined at the orifice boundaries (inlet, outlet, and wall) are approximated using a plasma density $\bar{n}$ averaged over the entire orifice volume. The particle flows in the HC orifice are shown in Fig. 2. The approach of the model is to define the equation of the motion of ions and neutrals in terms of averaged parameters to obtain a set of algebraic equations.

A. Neutral Gas Flow

The neutral gas flow velocity is obtained assuming Poiseuille flow:

$$\bar{u}_0 = \beta \frac{r^2 k_B T_0 \bar{n}_0}{4\xi L} \tag{1}$$

Received 26 July 2011; revision received 30 November 2011; accepted for publication 7 January 2012.

*Ph.D. Student, Physics Department; jorpalac@tx.technion.ac.il.
†Ph.D. Student, Physics Department; vladon@tx.technion.ac.il.
‡Senior Research Scientist, Physics Department; tsalevich@yahoo.com.
§Professor, Physics Department; fnkrasik@physics.technion.ac.il.

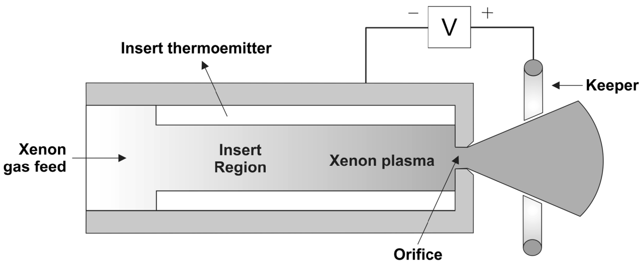

Fig. 1 Scheme of a hollow cathode.

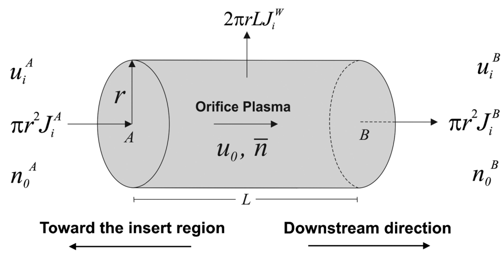

Fig. 2 Plasma parameters and fluxes in the orifice.

where $\beta = (1-\alpha)/(1+\alpha)$, the parameter $\alpha = n_0^B/n_0^A$ determines the decrease in pressure from the orifice inlet to the orifice outlet, $\bar{n}_0 = (n_0^A + n_0^B)/2$, and ξ is a function of T_0, which can be determined in the case of Xe gas as [1,2]:

$$\xi = 2.3 \times 10^{-5} T_r^{0.71+(0.29/T_r)}; \qquad T_r = T_0(°\mathrm{K})/289.7 \tag{2}$$

The variable α is a free parameter in this model. In the case of the NSTAR neutralizer HC, we consider the decrease in pressure from the orifice inlet to the outlet to be 80%, and then $\alpha = 0.2$, $\beta = 0.67$.

B. Ion Flux Across the Orifice Boundaries

The electron and ion momentum equation can be written as [2,3]:

$$J_e = eD_e \frac{\partial n}{\partial z} + en\mu_e E \tag{3}$$

$$nu_i = nu_0 - D_i \frac{\partial n}{\partial z} + n\mu_i E \tag{4}$$

Here, $D_i = eT_i/(M\nu_{\mathrm{in}})$, $D_a = (1 + T_e/T_i)D_i$, $\mu_e = e/(m(\nu_{\mathrm{ei}} + \nu_{\mathrm{en}}))$, and $\mu_i = e/(M\nu_{\mathrm{in}})$.

Combining Eqs. (3) and (4) results in

$$nu_i = nu_0 - D_a \frac{\partial n}{\partial z} \tag{5}$$

Here we neglected $(\mu_i J_e/\mu_e e)$ because $(\mu_i/\mu_e) = (m/M)[(\nu_{\mathrm{ei}} + \nu_{\mathrm{en}})/\nu_{\mathrm{in}}] \ll 1$. At low ion temperatures $\sigma_{\mathrm{CEX}} \gg \sigma_{\mathrm{in}}$ [4], and the ion charge-exchange collision becomes the dominant collision process, which makes it difficult for ions to diffuse because fast ions and slow neutrals exchange their identities, giving rise to slow ions that diffuse more slowly. Therefore, the relevant mean free path, collision frequency, and diffusion coefficient for ion—neutral interaction can be estimated as $\lambda_{\mathrm{in}} = \lambda_{\mathrm{CEX}} \approx (\bar{n}_0\sigma_{\mathrm{CEX}})^{-1}$, $\nu_{\mathrm{in}} \approx \bar{n}_0\sigma_{\mathrm{CEX}}\sqrt{eT_i/M}$, and $D_i \approx \lambda_{\mathrm{CEX}}^2 \nu_{\mathrm{in}}$, respectively.

It is expected that the plasma has a positive density gradient $(\partial n/\partial z)|_A \approx \bar{n}/(L/2)$ at the orifice inlet due to the larger ionization rate; at the orifice outlet, where the pressure is lower, the plasma obtains a negative density gradient $(\partial n/\partial z)|_B \approx -\bar{n}/(L/2)$. By applying Eq. (5) to the orifice inlet and outlet, one obtains

$$\bar{n}(u_i^{A,B} - u_0) = \mp D_a \frac{\bar{n}}{L/2} \tag{6}$$

Equation (6), along with the continuity equation applied at the inlet and outlet of the orifice $M\pi r^2[n_0^{A,B}u_0 + \bar{n}u_i^{A,B}] = F$, yields

$$M\pi r^2[\bar{n}_0 + \bar{n}]u_0 = F \tag{7}$$

The radial ion propagation is described as

$$J_i^w = -eD_a \frac{\partial n}{\partial r}\bigg|_{\mathrm{wall}} \approx eD_a \frac{\bar{n}}{r} \tag{8}$$

Finally, the axial ion propagation [see Eq. (6)] can be expressed as

$$J_i^{A,B} = e\bar{n}u_i^{A,B} \approx e\bar{n}u_0 \mp e\mathrm{D}_a \frac{\bar{n}}{L/2} \tag{9}$$

C. Ion Balance

The ion generation rate reads

$$I_i^{\mathrm{prod}} = L\pi r^2 e\bar{n}\bar{n}_0\langle\sigma_{\mathrm{ion}}u_e\rangle \tag{10}$$

The reaction rate $\langle\sigma_{\mathrm{ion}}u_e\rangle$ in Eq. (11) can be estimated as $\langle\sigma_{\mathrm{ion}}u_e\rangle \approx \langle\sigma_{\mathrm{ion}}\rangle\bar{u}_e$ for Xe gas for $T_e < 5$ eV [1,3], where $\bar{u}_e = [8eT_e(\mathrm{eV})/(\pi m)]^{1/2}$, and σ_{ion} averaged over a Maxwellian distribution of energy is a function of T_e:

$$\langle\sigma_{\mathrm{ion}}\rangle = (m/(2\pi k_B T_e))^{3/2} \iiint \sigma_{\mathrm{ion}}(u^2)\exp[-mu^2/(k_B T_e)]\,\mathrm{d}^3u = \sigma_{\mathrm{ion}}(T_e) \tag{11}$$

In [1] on pages 473–474, there is a table of experimental ionization cross-section data for Xe gas which are used to calculate $\langle\sigma_{\mathrm{ion}}\rangle$. A fitting of the results in the range $0.5\ \mathrm{eV} \le T_e \le 5\ \mathrm{eV}$ results in [1–3]

$$\sigma_{\mathrm{ion}}(T_e) \approx 10^{-20} \times [3.97 + 0.643T_e - 0.0368T_e^2]\exp(-U_{\mathrm{ion}}/T_e) \tag{12}$$

where T_e is given in eV, σ_{ion} in m^2, and $U_{\mathrm{ion}} = 12.13$ eV. The ion loss rate is given approximately by

$$I_i^{\mathrm{loss}} = \pi r^2(J_i^B - J_i^A) + 2\pi rLJ_i^W \tag{13}$$

where J_i^A has a negative sign because it is assumed to be directed toward the orifice. In fact, the results of calculations will determine its actual direction. Applying Eqs. (8), (9), and (13), one can determine the total (i.e., in radial and axial directions) ion current losses:

$$I_i^{\mathrm{loss}} \approx \frac{4\pi er^2 D_a\bar{n}}{L} + 2\pi LeD_a\bar{n} \tag{14}$$

In steady state, $I_i^{\mathrm{prod}} = I_i^{\mathrm{loss}}$, which leads to:

$$\bar{n}_0\sigma_{\mathrm{ion}}(T_e)\bar{u}_e = (2D_a/r^2)[1 + 2(r/L)^2] \tag{15}$$

D. Plasma Electron Energy Balance

In steady state, the joule heating of the plasma electrons compensates the electron energy loss due to ionization, excitation with radiative deexcitation, and convection [5,6]:

$$RI_e^2 = \pi r^2 L\bar{n}\bar{n}_0[\langle\sigma_{\mathrm{ion}}u_e\rangle eU_{\mathrm{ion}} + \langle\sigma_{\mathrm{rad}}u_e\rangle eU_{\mathrm{excit}}] + \frac{5}{2}(T_e - T_e^{\mathrm{ins}})I_e \tag{16}$$

In Eq. (16), the resistance

$$R = L\eta/(\pi r^2) = Lm(\nu_{\mathrm{ei}} + \nu_{\mathrm{en}})/(\pi r^2 e^2\bar{n}) = R_{\mathrm{ei}} + R_{\mathrm{en}}$$

takes into account electron—ion and electron—neutral atom collisions, where [1–3]: $\nu_{\mathrm{ei}} = 2.9 \times 10^{-12}\bar{n}T_e^{-3/2}\ln(\lambda_D/b_0)$, and $\nu_{\mathrm{en}} \approx \bar{n}_0\langle\sigma_{\mathrm{en}}u_e\rangle$, $\lambda_D = (\varepsilon_0 T_e/(e\bar{n}))^{1/2}$, $b_0 = e^2/(4\pi\varepsilon_0 m\bar{u}_e^2)$, and the reaction rates $\langle\sigma_{\mathrm{en}}u_e\rangle$ and $\langle\sigma_{\mathrm{rad}}u_e\rangle$ are estimated as:

$$\langle\sigma_{\mathrm{en}}u_e\rangle \approx \langle\sigma_{\mathrm{en}}\rangle\sqrt{eT_e/m} \approx 6.6 \times 10^{-19}[(0.25T_e - 0.1)/(1 + (0.25T_e)^{1.6})]\sqrt{eT_e/m}$$

and $\langle \sigma_{\rm rad} u_e \rangle \approx \langle \sigma_{\rm rad} \rangle \bar{u}_e \approx 1.93 \times 10^{-19} T_e^{-1/2} e^{-11.6/T_e} \bar{u}_e$, where T_e eV, σ in m^2, and $U_{\rm excit} \approx 10$ eV.

E. Comparison Between Two 0-D Models

A 0-D model permits only averaged plasma parameters to be calculated. In Mandell and Katz's [5] and Katz et al.'s [6] 0-D model, the plasma parameter gradients within the orifice were neglected and, therefore, the plasma flow was not considered. Thus, to explain the flux of particles across the orifice boundaries, the thermal motion of the plasma particles was used in their model. However, by definition such fluxes are symmetrical in all of the directions, giving rise to no net plasma displacement. The present new model takes the gradients of the plasma parameters within the orifice into account; to obtain a 0-D model, the gradients are estimated as quotients between average values of the parameters and the orifice radius and length. In Table 1 the differences between the two models are summarized.

In the Mandell and Katz and Katz et al. model, the plasma ions have a Maxwellian distribution with the electron temperature [5,6]. This assumption implies either that the neutrals also have electron temperature, which is actually unrealistic (see Sec. III) or neutrals are much cooler than ions, which is also unrealistic due to ion—neutral high collisionality within the orifice. The new model uses a more realistic assumption: $T_0 = T_i < T_e$.

III. Analysis of the Energy Transfer Due to Electron—Ion and Electron—Neutral Collisions

The total energy per second per unit of volume that is transferred from the electrons to neutral atoms and ions through collisions are given, respectively, by:

$$Q_{\rm ei} = \nu_{\rm ei} \bar{n} \frac{2m}{M} \frac{3}{2} e(T_e - T_i) \tag{17}$$

$$Q_{\rm en} = \nu_{\rm en} \bar{n} \frac{2m}{M} \frac{3}{2} e(T_e - T_0) \tag{18}$$

Assuming $T_i = T_0$, the total energy exchange rate per unit of volume is

$$Q_{\rm total} = (\nu_{\rm ei} + \nu_{\rm en}) \bar{n} \frac{2m}{M} \frac{3}{2} e(T_e - T_i) \tag{19}$$

The drift velocity of the plasma electrons propagating through the orifice is $u_e^d = I_e/(en\pi r^2)$, and the average propagation time of the electrons through the orifice is $\tau = L/u_e^d = en\pi r^2 L/I_e$. The total energy density transferred from the electrons to the heavy species during electron propagation through the orifice is $Q_{\rm total}\tau$. The specific heat capacity for Xe atoms or ions considered as a monoatomic ideal gas is $c_v = 3\tilde{R}/(2m_{\rm Xe}) = 95$ J/(kg °K), where $\tilde{R} = 8.31$ J/(°K mol) and $m_{\rm Xe} = 0.1313$ kg/mol. The total density of the heavy particles is $\rho_{\rm total} = M(n_0 + n)$. Thus, the total heat capacity per unit of volume is $c_{\rm total} = \rho_{\rm total} c_v = M(n_0 + n)c_v$. One can now estimate the increase in the heavy species temperature as

$$\Delta T[{\rm eV}] = \frac{k_B}{e} \frac{Q_{\rm total}\tau}{c_{\rm total}} = \frac{k_B}{e} \frac{[(\nu_{\rm ei} + \nu_{\rm en}) n \frac{2m}{M} \frac{3}{2} e(T_e - T_i)](en\pi r^2 L/I_e)}{M(n_0 + n)c_v} \tag{20}$$

Equation (20) does not include interactions of heavy particles with the orifice wall and considers only the increment in temperature of heavy particles due to electron collisions. For instance, for the NSTAR neutralizer HC (see Sec. IV) the increase in temperature will be only $\Delta T = 0.045$ eV. This allows one to conclude that collisions between the heavy species and the plasma electrons within the orifice are not enough for those particles to reach thermal equilibrium.

IV. Results of the Model

The model was applied to the NSTAR neutralizer HC [1,2,7], which has dimensions $L = 0.75$ mm, $r = 0.14$ mm. Because the plasma parameters within this HC have not been measured, we present a comparison with the predictions of other models. The ion and neutral gas temperature is taken to be $T_i = T_0 = 0.4$ eV [7]. The calculated viscosity is $\xi = 1.7 \times 10^{-4}$ Pa·s, which results in a Reynolds number $Re < 10$, implying that the flow is laminar. The application of the model is restricted to HCs with a large aspect ratio $L/(2r) > 1$ and orifices with $r \leq 0.3$ mm, for which the assumption of Poiseuille flow can be applied. The operation conditions of the HC are Xe gas flow rate $F = 3.6$ sccm $= 0.354$ mg/s and discharge current $I_e = 3.26$ A. The results of the calculations are reported in Table 2.

One can see that the neutral density value predicted by the 0-D model of Mandell and Katz and Katz et al. [5,6] is closer to the values predicted by the two-dimensional (2-D) model than is the value

Table 1 Differences between the two 0-D models

0-D new model	0-D model (Mandell and Katz [5])
1 Plasma flowing along the orifice.	1 Plasma static and homogeneous within the orifice.
2 The flux of particles across the orifice boundaries is determined by hydrodynamic forces. In particular viscous forces are taken into account.	2 The flux of particles across the orifice boundaries is due to thermal motion. Viscous effects are completely neglected.
3 Plasma ions can be dragged by the neutral gas flow from the insert region toward the orifice region depending on the mass flow rate fed to the HC.	3 Plasma ions flow out of the orifice symmetrically in both directions, namely, downstream to the outside of the HC and upstream toward the insert region.
4 Neutral atoms and plasma ions have the same temperature, which in turn is lower than the plasma electron temperature: $T_0 = T_i < T_e$.	4 Plasma electrons and ions have the same temperature, while neutral atoms could be cooler: $T_0 \leq T_i = T_e$.

Table 2 Comparison of the plasma parameters predicted by different models for the NSTAR neutralizer HC

	0-D model (our model)	0-D model (Mandell and Katz [5] and Katz et al. [6])	1-D model (Katz et al. [2])			2-D model (Mikellides and Katz [7])		
Plasma parameters	Average	Average	Orifice inlet	Maximum reached value	Orifice outlet	Orifice inlet	Maximum reached value	Orifice outlet
$n_0(10^{23}$ m$^{-3})$	1.1	0.4	2.8	2.8	0.6	0.65	0.65	0.1
$n(10^{22}$ m$^{-3})$	2.7	1.0	2.8	6.0	1.8	2.0	2.2	0.5
T_e (eV)	1.6	2.2	1.2	1.8	1.8	2.0	2.2	2.2
$\frac{n}{n+n_0}$	0.20	0.18	0.09	0.24	0.23	0.23	0.50	0.33

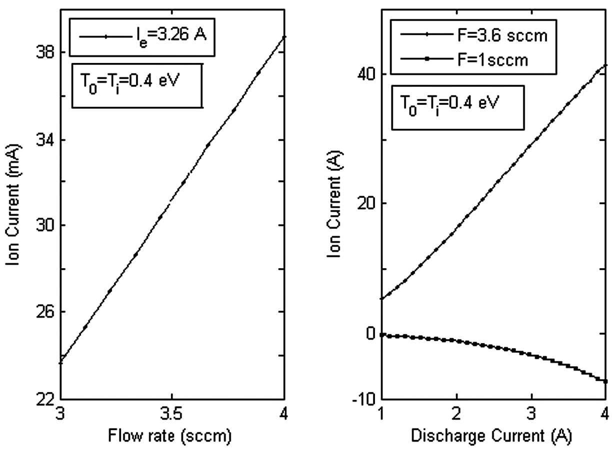

a) b)

Fig. 3 Dependence of the ion current at the orifice inlet vs a) Xe gas flow rate, and b) discharge current.

predicted by the new 0-D model. However, the former two models do not take the gas viscosity into account [5–7], and, as Mikellides and Katz remark in [7], the viscosity effect increases the inner pressure (by about 50%) of the HC and, respectively, the neutral density. Notice that there is better agreement between the new 0-D model and the one-dimensional (1-D) model because both take the gas viscosity into account. Also, the value of T_e decreases with the increase in n_0. Thus, when viscous effects are taken into account, the calculated value of n_0 increases while T_e decreases, as can be seen from the results of the new 0-D model and the 1-D model.

Following the assumption of the Mandell and Katz and Katz et al. [5,6] model that $T_i = T_e$, one obtains a neutral gas temperature also of $T_0 = 2.2$ eV, which is a very high temperature for neutrals. However, if one considers the value of T_0 in the range 0.18 eV–0.38 eV calculated by the 2-D model [7], then, following Mandell and Katz' and Katz et al.'s 0-D model, one obtains $T_i = T_e = 1.9$ eV, which is far from equilibrium with neutrals. This inconsistency is absent in the new model. Also, one can see that the plasma density and ionization degree predicted by the new 0-D model are in better agreement with the values predicted by the 1-D and 2-D models than with the corresponding value predicted by the 0-D model of Mandell and Katz and Katz et al.

An additional feature is that the new 0-D model predicts that the neutral gas flow drags the ions from the insert region toward the orifice, and only when the neutral flow rate fed to the HC is low (≤ 1 sccm) do the ions flow in the upstream direction from the orifice to the insert region (see Fig. 3, where negative values of the ion current at the orifice inlet means ion flow in the upstream direction). This agrees very well with the results of the 2-D model (see Fig. 12 in [7]). Here let us note that in Katz et al.'s 0-D model it was supposed that the ions at the orifice inlet flow only in the upstream direction [5,6], which agrees with Katz et al.'s 1-D model [2], where this ion flow direction was obtained as the result of calculations, but is in contradiction with the 2-D model results [7]. However, our simplified 0-D model, the implementation of which is much faster than that of the 1-D or 2-D models, predicts plasma parameters in agreement with the results of a 2-D model [7].

V. Conclusions

A proposed 0-D model for the plasma within the orifice of HCs has been presented. A comparison of the results of this model with those obtained by one-dimensional and two-dimensional models reveals a better agreement than that obtained with the earlier 0-D model. The analysis of the energy transfer from the plasma electrons to ions and neutral atoms within the orifice showed that the heavy plasma species cannot reach thermal equilibrium with the plasma electrons, justifying the assumption $T_0 = T_i < T_e$. Also, it was found that the direction of the ion flow at the orifice input depends strongly on the rate of the neutral flow.

Acknowledgment

Special thanks are for Ehud Behar for useful discussions.

References

[1] Goebel, D., and Katz, I., *Fundamentals of Electric Propulsion*, Wiley, NY, 2008, pp. 58, 463–466.

[2] Katz, I., Anderson, J. R., Polk, J. E., and Brophy, J. R., "One-Dimensional Hollow Cathode Model," *Journal of Propulsion and Power*, Vol. 19, No. 4, July–Aug. 2003, pp. 595–600. doi:10.2514/2.6146

[3] Katz, I., Anderson, J. R., Polk, J. E., and Brophy, J. R., "A Model of Hollow Cathode Plasma Chemistry," AIAA Paper 2002-4241, July 2002.

[4] Miller, J. S., Pullins, S. H., Levandier, D. J., Chiu, Y.-H., and Dressler, R. A., "Xenon Charge Exchange Cross Sections for Electrostatic Thruster Models," *Journal of Applied Physics*, Vol. 91, No. 3, Feb. 2002, pp. 984–991. doi:10.1063/1.1426246

[5] Mandell, M., and Katz, I., "Theory of Hollow Cathode Operation in Spot and Plume Modes," AIAA Paper 1994-3134, Oct. 1994.

[6] Katz, I., Gardner, B. M., Mandell, M. J., Jongeward, G. E., Patterson, M., and Myers, R. M., "Model of Plasma Contactor Performance," *Journal of Spacecraft and Rockets*, Vol. 34, No. 6, Nov.–Dec. 1997, pp. 824–828. doi:10.2514/2.3294

[7] Mikellides, I., and Katz, I., "Wear Mechanisms in Electron Sources for Ion Propulsion, 1: Neutralizer Hollow Cathode," *Journal of Propulsion and Power*, Vol. 24, No. 4, July–Aug. 2008, pp. 855–865. doi:10.2514/1.33461

L. King
Associate Editor